European Journal of Pharmaceutical Sciences 117 (2018) 98–106

Contents lists available at ScienceDirect

European Journal of Pharmaceutical Sciences

journal homepage: www.elsevier.com/locate/ejps

A reaction limited *in vivo* dissolution model for the study of drug absorption: Towards a new paradigm for the biopharmaceutic classification of drugs

Panos Macheras[a,b,*], Athanassios Iliadis[c], Georgia Melagraki[d]

[a] Laboratory of Biopharmaceutics–Pharmacokinetics, Department of Pharmacy, School of Health Sciences, National and Kapodistrian University of Athens, Athens, Greece
[b] Pharmainformatics Unit "Athena" Research and Innovation Center, Athens, Greece
[c] Aix Marseille University, SMARTc, INSERM CRO2 UMR_S911, Marseille, France
[d] Department of Military Sciences, Division of Physical Sciences and Applications, Hellenic Army Academy, Vari, Greece

ARTICLE INFO

Keywords:
Reaction limited model
Dissolution
Solubility
Supersaturation
BCS
BDDCS

ABSTRACT

The aim of this work is to develop a gastrointestinal (GI) drug absorption model based on a reaction limited model of dissolution and consider its impact on the biopharmaceutic classification of drugs. Estimates for the fraction of dose absorbed as a function of dose, solubility, reaction/dissolution rate constant and the stoichiometry of drug-GI fluids reaction/dissolution were derived by numerical solution of the model equations. The undissolved drug dose and the reaction/dissolution rate constant drive the dissolution rate and determine the extent of absorption when high-constant drug permeability throughout the gastrointestinal tract is assumed. Dose is an important element of drug-GI fluids reaction/dissolution while solubility exclusively acts as an upper limit for drug concentrations in the lumen. The 3D plots of fraction of dose absorbed as a function of dose and reaction/dissolution rate constant for highly soluble and low soluble drugs for different "stoichiometries" (0.7, 1.0, 2.0) of the drug-reaction/dissolution with the GI fluids revealed that high extent of absorption was found assuming high drug- reaction/dissolution rate constant and high drug solubility. The model equations were used to simulate *in vivo* supersaturation and precipitation phenomena. The model developed provides the theoretical basis for the interpretation of the extent of drug's absorption on the basis of the parameters associated with the drug-GI fluids reaction/dissolution. A new paradigm emerges for the biopharmaceutic classification of drugs, namely, a model independent biopharmaceutic classification scheme of four drug categories based on either the fulfillment or not of the current dissolution criteria and the high or low % drug metabolism.

1. Introduction

From the first physicochemical dissolution experiment in 1897 to the mid-50s when dissolution was introduced in drug research, the question associated with the mechanism of dissolution process attracted the interest of many physicochemical scientists (Dokoumetzidis and Macheras, 2006; Higuchi, 1967; Macheras and Iliadis, 2016). The dilemma of diffusion- or reaction-limited dissolution was then transferred in 50s to the pharmaceutical field with two additional, important and interconnected aspects for the drug dissolution experiments: i) the relation of the agitation rates of the (official) dissolution tests with the dissolution mechanism(s) and ii) the relevance of the *in vitro* agitation conditions with the conditions in the gastrointestinal (GI) lumen and the associated correlations between the *in vitro* and *in vivo* dissolution data. The latter aspect progressively gained popularity since: i) dissolution was increasingly used as a surrogate for bioavailability, ii) food mimicking and biorelevant media were utilized in drug dissolution studies to emulate the fed or fasted state and iii) *in vitro-in vivo* correlations (IVIVC) were developed (Cardot and Davit, 2012; González-García et al., 2015; Klein, 2010; Macheras et al., 1986).

A MEDLINE search reveals that the first physicochemical studies in the literature, using the search terms 'solubilization AND drug', 'supersaturation AND drug' or 'supersaturation AND dissolution', were published in 1966, 1974 and 1976, respectively (Anderson and Morgan, 1966; Griffith et al., 1976; Holzbach and Pak, 1974). For half a century now all these terms are found in dissolution studies dealing with solid dispersion formulations, drug coprecipitates with water-soluble polymers (*e.g.* hydroxylpropylmethyl-cellulose, polyvinylpyrrolidone or polyethylene glycol *etc.*), as well as classical or micellar solubilization approaches using artificial surfactants (*e.g.* sodium lauryl sulfate) or biosurfactants (*e.g.* bile salts). The main scope of these studies and many others of similar nature is to improve the bioavailability of drug as a result of the enhancement of solubility and/or the dissolution rate. Although the fast dissolution rate is attributed to either a high energy

* Corresponding author at: Laboratory of Biopharmaceutics–Pharmacokinetics, Department of Pharmacy, National and Kapodistrian University of Athens, Athens 15784, Greece.
E-mail address: macheras@pharm.uoa.gr (P. Macheras).

https://doi.org/10.1016/j.ejps.2018.02.003
Received 8 November 2017; Received in revised form 19 December 2017; Accepted 5 February 2018
Available online 06 February 2018
0928-0987/

coprecipitate (de Ilarduya et al., 1998) or to the various amorphization strategies (Cheow et al., 2014; Li et al., 2014; Vrbata et al., 2014), the reaction limited dissolution model (RLMD) is neither implied nor modeled in the studies. However, the rapidity of drug dissolution at the early stages in many of these studies does not fit with the diffusion principles; on the contrary, a very rapid initial dissolution rate indicates that a 'rapid reaction' has taken place between the drug's solid particles and the species/components of the dissolution medium.

As a matter of fact, the diffusion limited dissolution mechanism is considered as the prevailing mechanism of drug dissolution since early 60s. Classical pharmaceutics and biopharmaceutics books published in 70s and 80s do not even quote a hint for the RLMD. The prevalence of the diffusion limited dissolution mechanism is mainly due to the theoretical work of Levich (Levich, 1962) on diffusion kinetics in the liquid phase using a rotating disk dissolution apparatus under fully controlled hydrodynamic conditions. According to the diffusion layer model, the general expression for the rate of drug dissolution is:

$$\frac{dC}{dt} = k(C_s - C) \tag{1}$$

where C is the drug concentration at time t, C_s is the solubility of drug in the studied medium and k is a composite first-order constant. Eq. (1) reveals that dissolution is a passive process and the saturation solubility drives the dissolution rate. However, the assumptions associated with the diffusion layer model of drug dissolution have been considered unphysical (Wang et al., 2012); in fact, the view of a constant layer thickness is an over simplification since modern hydrodynamics studies show that this layer is a function of the Sherwood number. Besides, the application of the ideal assumptions for a Fickian-type diffusion limited dissolution under *in vivo* conditions has been questioned (Macheras and Argyrakis, 1997). This study places emphasis on the hydrodynamic situation in a compendial *in vitro* test *versus* an expected *in vivo* dissolution; it introduces the concept of homogenous stirring conditions of the *in vitro* tests due to the re-randomization of drug species and the heterogeneous conditions prevailing *in vivo* because of the insufficient stirring. An extensive discussion for the limitations of the diffusion layer model, along with the development of a reaction limited model of dissolution and its application to supersaturated dissolution curves can be found in the literature (Charkoftaki et al., 2011; Dokoumetzidis et al., 2008).

Another piece of evidence in favor of RLMD has been observed in the course of dissolution studies (Crisp et al., 2007; Dokoumetzidis et al., 2008). The study (Crisp et al., 2007) clearly demonstrates that the interfacial reaction at the drug's surface becomes dominant when the nanoparticles of danazol and itraconazole smaller than 1 μm were examined. In the study (Dokoumetzidis et al., 2008), the models based on functions associated with the diffusion layer model failed to reveal the governing role, of the saturation solubility for the dissolution process. However, one recent article on the theoretical analysis of drug dissolution focuses on the question "how important a reaction limited is as opposed to a diffusion limitation?" (Shekunov and Montgomery, 2016). This study shows that both mechanisms can matter and each mechanism may prevail depending on the specific situation given. For example, the contribution of the reaction limited mechanism becomes more dominant when the surface kinetic coefficient may decrease as a function of solution composition.

The development of Biopharmaceutics Classification System (BCS) (Amidon et al., 1995) and relevant software dealing with GI absorption rely on Eq. (1) for the description of *in vivo* drug dissolution. According to Eq. (1), a monotonic exponential increase of drug concentration towards the saturation solubility as a function of time is anticipated in dissolution studies. However, is not uncommon to see supersaturated dissolution curves in *in vitro* and *in vivo* studies (Brouwers et al., 2009), while the associated concept 'kinetic solubility'(Box and Comer, 2008) is increasingly used in the field and drug precipitation phenomena are frequently observed and studied under *in vivo* conditions (Jakubiak et al., 2016; Khan et al., 2016).

The aim of this work is to formulate a reaction limited dissolution model (RLMD) for the study of gastrointestinal absorption of drugs. Furthermore, the impact of RLMD on the biopharmaceutic classification of drugs is explored.

2. Materials and methods

The RLMD developed (Dokoumetzidis et al., 2008) relies on the bidirectional chemical reaction with microconstants k_1 and k_{-1} at the solid-liquid interface of the undissolved drug species (s) with n free species/components of the dissolution medium (w), yielding the dissolved species of drug complex with solvent c:

$$s + nw \underset{k_{-1}}{\overset{k_1}{\rightleftarrows}} c \tag{2}$$

The unidirectional case of Eq. (2) implies sink conditions and corresponds to a complete dissolution of drug dose while the more general case of the bidirectional reaction corresponds to saturation of solution *i.e.* the reaction reaches chemical equilibrium. Assuming that the molar concentration of the solvent species w can be considered equal to the initial concentration w_0 of the free solvent species, the rate of dissolution, expressed in terms of drug concentration, C in mass/volume units is as follows (Dokoumetzidis et al., 2008):

$$\frac{dC}{dt} = k_1^* \left(\frac{D}{V} - C\right)^{\alpha} - k_{-1}C \tag{3}$$

where $k_1^* = k_1[w_0]^b$ (molecular weight of the complex $c)^{1-\alpha}$, α, b are exponents that determine the order of the reaction, D is the initial quantity (dose) in mass units and V is the volume of the dissolution medium.

Eq. (3) reveals that the rate of dissolution is driven by the concentration of the undissolved species and not the saturation solubility implied in the diffusion layer model of dissolution (Eq. (1)). Interestingly, the saturation solubility C_s in the RLMD model corresponds to the concentration when the reaction equilibrium is reached *i.e.* C_s is equal to the concentration at the steady state C_{ss} when the drug dose D is in excess (Dokoumetzidis et al., 2008):

$$Css = \frac{k_1^*}{k_1^* + k_{-1}}\frac{D}{V} \tag{4}$$

Moreover, Eq. (3) was proven (Dokoumetzidis et al., 2008) not only capable in mimicking the dissolution profiles of classic equations based on the diffusion layer model but also it exhibited additional flexibility. Most importantly, a modified version of Eq. (3) using a time dependent expression for k_1 * nicely described supersaturated experimental dissolution data of carbamazepine in presence of D-alpha–tocopheryl polyethylene glycol 1000 succinate (Charkoftaki et al., 2011):

$$k_1^* = K(\lambda + (1 + t)^{-h}) \tag{5}$$

where K is a constant in $(\text{time})^{h-1}$ units, h is a unit less number and λ is a constant in $(\text{time})^{-h}$ units, preventing the entire expression from approaching zero for large times.

Supersaturated dissolution curves have been also observed in dissolution studies with sparingly soluble compounds (Parikh et al., 2016; Verma and Rudraraju, 2015). A quite relevant term, 'wetting kinetics' has been coined (Verma and Rudraraju, 2015). Similarly, supersaturated dissolution data whereas metastable forms are gradually transformed to the most stable physical form have been observed (Greco and Bogner, 2012; Pouton, 2006). Due to the monotonic nature of Eq. (1), all these cases cannot be explained with Eq. (1) while the RLMD relies on a 'reaction' concept and seems to capture the dynamics of the classical dissolution data as well as the supersaturated dissolution data (Charkoftaki et al., 2011).

2.1. Consideration of RLMD under in vivo conditions

The current biopharmaceutic classification guideline (FDA, 2015) relies on solubility and permeability values. The use of solubility arises from the use of diffusion layer model to emulate drug dissolution in the fundamental articles of the gastrointestinal drug absorption (Amidon et al., 1995; Oh et al., 1993). In the same vein, the RLMD can be also considered under *in vivo* conditions. One can write the equation of drug dissolution-uptake in a manner similar to that used for the development of BCS (Amidon et al., 1995; Oh et al., 1993) assuming the same homogeneous tube model:

$$\frac{dC_L}{dt} = k_1^* \cdot \left(\frac{D}{V} - C_L\right)^{\alpha} - k_{-1} \cdot C_L - \frac{2 \cdot P_{eff}}{R} \cdot C_L \tag{6}$$

where C_L is the concentration of dissolved drug in the intestinal lumen, P_{eff} is the effective permeability of the drug and R is the tube radius.

Visual inspection of Eq. (6) reveals the two parameters controlling oral drug absorption, namely, the dissolution rate constant k_1^* for the reaction of the undissolved drug species with the fluids and/or components of the gastrointestinal lumen and the drug permeability, P_{eff}. It should be emphasized that the undissolved drug mass (expressed in terms of concentration, $\frac{D}{V} - C_L$) drives the dissolution rate while the uptake is assumed to follow the classical passive diffusion pathway.

2.1.1. Model development

The proper mathematical treatment of the fundamental dissolution-reaction (Eq. (2)) and the corresponding reaction/dissolution/uptake (Eq. (6)) require molecular concentrations and knowledge of the stoichiometry (α) of the dissolution-reaction. However, the use of molecular concentrations in the complex-unstirred GI fluids is inappropriate; moreover, the stoichiometry of the reaction is unknown while the exponent α is also associated with the geometry and roughness of the solid particles. This means that the exponent α can take both integer and non-integer values (Valsami and Macheras, 1995). For all above reasons, the model used for the drug dissolution-uptake for a given dose D was based on the amount of undissolved, dissolved and absorbed drug, $q_U(t)$, $q_L(t)$ and $q_A(t)$, respectively. The rate of variation of these amounts is given by the following differential equations

$$\begin{aligned} \dot{q}_U(t) &= -k_1^* \cdot q_U(t)^{\alpha} + k_{-1} \cdot q_L(t) && q_U(0) = D \\ \dot{q}_L(t) &= k_1^* \cdot q_U(t)^{\alpha} - k_{-1} \cdot q_L(t) - (2 \cdot P_{eff}/R) \cdot q_L(t) && q_L(0) = 0 \\ \dot{q}_A(t) &= (2 \cdot P_{eff}/R) \cdot q_L(t) && q_A(0) = 0 \end{aligned} \tag{7}$$

The system of equations above describes three processes:

i) the rate of drug dissolution is equal to $k_1^* \cdot q_U(t)^{\alpha}$, where k_1^* is the dissolution rate constant (expressed in amount$^{1-\alpha} \cdot$ time^{-1} units) for the reaction of the undissolved drug species with the fluids and/or components of the gastrointestinal lumen; the exponent α is dimensionless and accounts for the stoichiometry/heterogeneous conditions in drug dissolution. In the homogeneous case $\alpha = 1$,
ii) the rate of drug precipitation $k_{-1} \cdot q_L(t)$, where k_{-1} is the rate constant of precipitation, and
iii) the rate of drug absorption $(2 \cdot P_{eff}/R) \cdot q_L(t)$, where P_{eff} and R are the effective drug permeability and the tube radius, respectively.

Moreover, the solubility C_S constraints the amount of dissolved drug $q_U(t)$ to be lower than $C_S \cdot V$, where V is the volume of the tube. Thus, the set of differential Eq. (7) is constrained at any time t by the inequality

$$q_L(t) \leq C_S \cdot V \tag{8}$$

Given the mass-balance equation, $D = q_U(t) + q_L(t) + q_A(t)$, the set of differential equations becomes

$$\begin{aligned} \dot{q}_L(t) &= k_1^* \cdot [D - q_L(t) - q_A(t)]^{\alpha} - k_{-1} \cdot q_L(t) - (2 \cdot P_{eff}/R) \cdot q_L(t) && q_L(0) = 0 \\ \dot{q}_A(t) &= (2 \cdot P_{eff}/R) \cdot q_L(t) && q_A(0) = 0 \end{aligned} \tag{9}$$

By integrating the last differential equation, the fraction of dose absorbed $F_a(t)$ up to time t is given by

$$F_a(t) = q_A(t)/D = (2 \cdot P_{eff}/R)/D \cdot \int_0^t q_L(\tau) \cdot d\tau \tag{10}$$

2.1.2. Simulation work

We used the Eqs. (7)–(10) quoted above, to estimate $F_a(t)$ and simulate the *in vivo* drug processes. For simulation purposes, $F_a(t)$ is considered for the mean intestinal transit time $t = MITT \approx 199$ min (Yu et al., 1996). A high permeable drug with absorption number $A_n = 10$ (Oh et al., 1993) was considered; this value corresponds to $P_{eff} = 0.050$ cm/ min . The half-life of the precipitation process was set at 14 min leading to $k_{-1} = 0.050$ min^{-1}; typical values $R = 1$ cm and $V = 250$ mL were used. Also, two solubility values were used $C_S = 1$ and 0.05 mg/mL. The set of Eqs. (8) and (9) was solved numerically to estimate $F_a(MITT)$ from Eq. (10) for values of k_1^* ranging from 10^{-4} to 10^{-1}mg$^{1-\alpha} \cdot$ min^{-1} and for values of D ranging from 100 to 1000 mg. Simulations were performed using integer (1 and 2) and non-integer (0.7) values for α. The parameters values 1 and 2 are the most plausible values for the stoichiometry of the reaction. The simplest, homogeneous case ($\alpha = 1$) corresponds to a well-mixed dispersion with the drug solid particles exhibiting the same probability to react (dissolve) with the solvent species. The use of a non integer value *i.e.* 0.7 relies on the concept of fractal reaction kinetics developed by R. Kopelman in his seminal article on fractal reaction kinetics (Kopelman, 1988). In this context, the "heterogeneous" reactions, when the reactants are spatially constrained on the microscopic level by phase boundaries (*e.g.* solid particle surface-GI fluids), exhibit fractal orders for elementary reactions and rate coefficients with temporal "memories". This work (Kopelman, 1988) emphasizes the importance of the size-topology-fractal dimension of the sample for heterogeneous reactions and the violation of old Wenzel's law (Wenzel, 2009), which states that the larger the interface, the faster the reaction. In addition, this article (Kopelman, 1988) plays particular emphasis on the "active" part of the surface and the relevant non-integer fractal dimension of the surface of the solid particles. These concepts were introduced in biopharmaceutics-pharmacokinetics by (Macheras and Argyrakis, 1997). Since then a plethora of fractal kinetics and most recently fractional kinetics papers were published in biopharmaceutics-pharmacokinetics literature focusing among other topics on the heterogeneity of drug dissolution (Macheras and Dokoumetzidis, 2000), drug absorption (Dokoumetzidis and Macheras, 2009) and nonlinear IVIVC (Kytariolos et al., 2010), most of which have been included in a book (Macheras and Iliadis, 2016).

We also generated the amount and time profiles for the undissolved, dissolved, and absorbed drug species by assigning the following values: $D = 200$ mg, $k_{-1} = 0.050$ min^{-1}, $k_1^* = 0.1$ mg$^{1-\alpha} \cdot$ min^{-1}, $C_S = 1$ mg/mL, for a low permeable drug with $P_{eff} = 0.001$ cm/min. A set of simulations were also performed to demonstrate that the model captures the dynamics of drug supersaturation and precipitation phenomena.

3. Results

The simulation results are shown in Figs. 1, 2 and 3 for the cases $\alpha = 1$, 2 and 0.7, respectively using a relatively soluble drug ($C_S = 1$ mg/mL) and an insoluble drug ($C_S = 0.05$ mg/mL) as model drugs.

The top plot of Fig. 1 for $\alpha = 1$ and $C_S = 1$ mg/mL demonstrates that the increase of $F_a(MITT)$ for all doses considered is proportional to the increase of reaction/dissolution rate constant k_1^*. Extensive

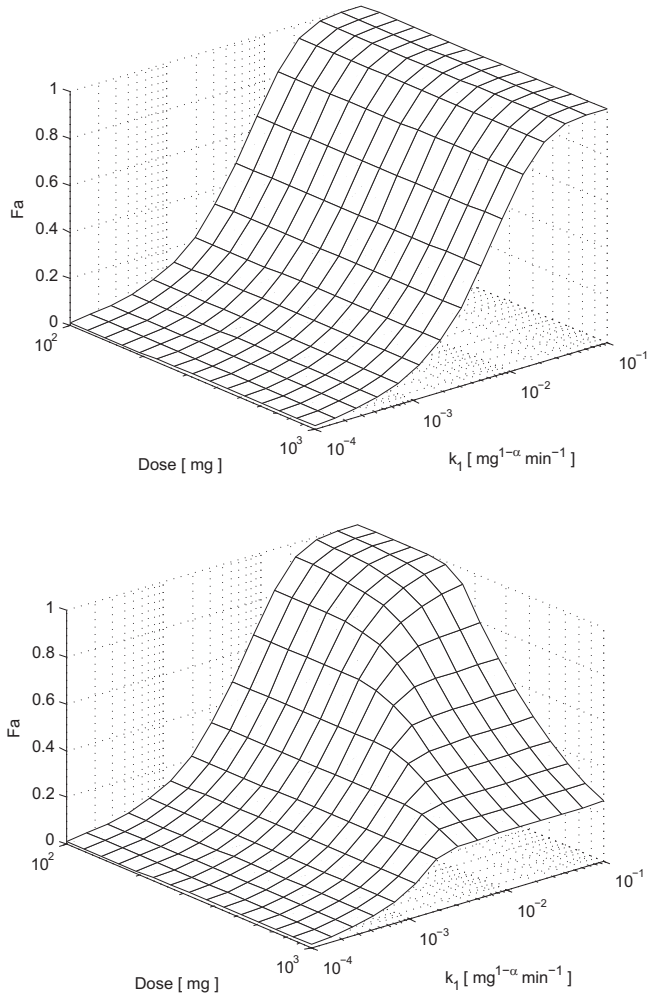

Fig. 1. Simulations of $F_a(MITT)$ with $\alpha = 1$ as a function of k_1^* and D with $C_S = 1$ (top) and 0.05 mg/mL (bottom).

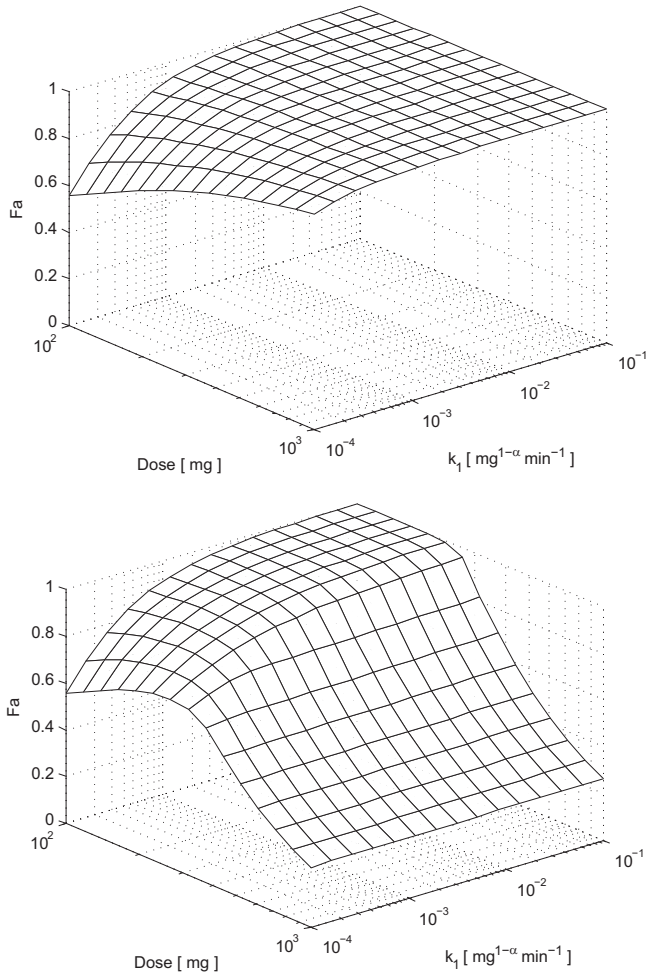

Fig. 2. Simulations of $F_a(MITT)$ with $\alpha = 2$ as a function of k_1^* and D with $C_S = 1$ (top) and 0.05 mg/mL (bottom).

absorption ($F_a(MITT) > 90\%$) is observed for $k_1^* > 0.015$ min^{-1}. On the contrary, the bottom plot of Fig. 1 for an insoluble drug ($C_S = 0.05$ mg/mL) and $\alpha = 1$ shows that extensive absorption is observed only for low drug doses and k_1^* close to the assigned maximum 0.1 min^{-1}.

A different pattern is observed at the top of Fig. 2 for $\alpha = 2$ and $C_S = 1$ mg/mL. Extensive absorption is observed for all k_1^* values considered but only for high drug doses, namely, close to the maximum dose assigned 1000 mg. For low drug doses, $F_a(MITT)$ increases with k_1^* (top of Fig. 2). This behavior is associated with the predominant role of the squared term in brackets of Eq. (9) in determining the drug dissolution rate. For a low soluble drug, the bottom plot of Fig. 2 shows that extensive absorption is observed for low drug doses and high k_1^* values. When the dose is increased above its lowest value 100 mg, $F_a(MITT)$ is also increasing with k_1^*. However, the values of $F_a(MITT)$ decrease steeply for $D > 250$ mg and all k_1^* values considered due to solubility limitations (bottom of Fig. 2).

The results shown in Fig. 3 with $\alpha = 0.7$ have a similar pattern to that shown in Fig. 1; however, $F_a(MITT)$ values in Fig. 3 are lower compared to the corresponding results presented in Fig. 1 for all cases examined since the exponent 0.7 of the term in brackets of Eq. (9) slows down the drug dissolution rate.

Figs. 4, 5 and 6 show the amount, time profiles for the undissolved, dissolved and absorbed drug for the relatively soluble drug ($C_S = 1$ mg/mL), with low permeability ($P_{eff} = 0.001$ cm/min) and by assigning α values equal to 0.7, 1 and 2, respectively. The above simulations were obtained with $D = 200$ mg, $k_{-1} = 0.050$ min^{-1} and $k_1^* = 0.1$ mg$^{1-\alpha} \cdot$ min^{-1}.

Fig. 7 demonstrates the impact of the rate constant k_{-1}, which governs the rate of drug precipitation, on the undissolved, dissolved and absorbed drug, time profiles. Fig. 8 shows two cases associated with supersaturation and precipitation phenomena.

4. Discussion

The results of Figs. 1 to 3 indicate that the solubility acts as an upper cutoff limit for the lumen drug concentration values. Solubility does not have a leading role in driving the dissolution rate (see the model Eqs. (9) and (10)) as it happens to be the case in the diffusion limited model of drug dissolution. The driving force of dissolution rate is the undissolved amount of drug (see the model Eq. (9)); therefore, the principal elements of the reaction/dissolution of drug with the GI fluids/components, namely, the reaction/dissolution rate constant k_1^*, the dose D, and the stoichiometry α determine the final estimate of $F_a(MITT)$.

Figs. 4, 5 and 6 demonstrate the expected shape for all curves, namely, a continuous decrease as a function of time for $q_U(t)$, a monotonic increase as a function of time for $q_A(t)$ while $q_L(t)$ is increasing initially reaching a maximum and then decreases gradually. Also, Figs. 4 to 6 demonstrate that the increase of α results in higher $q_L(t)$, lower $q_U(t)$ and higher $q_A(t)$ time profiles since all other parameters are the same. It should be noted that the case $\alpha = 0.7$ in Fig. 4 corresponds to “fractal kinetics” which has been observed in dissolution studies in biorelevant media (Niederquell and Kuentz, 2014). The

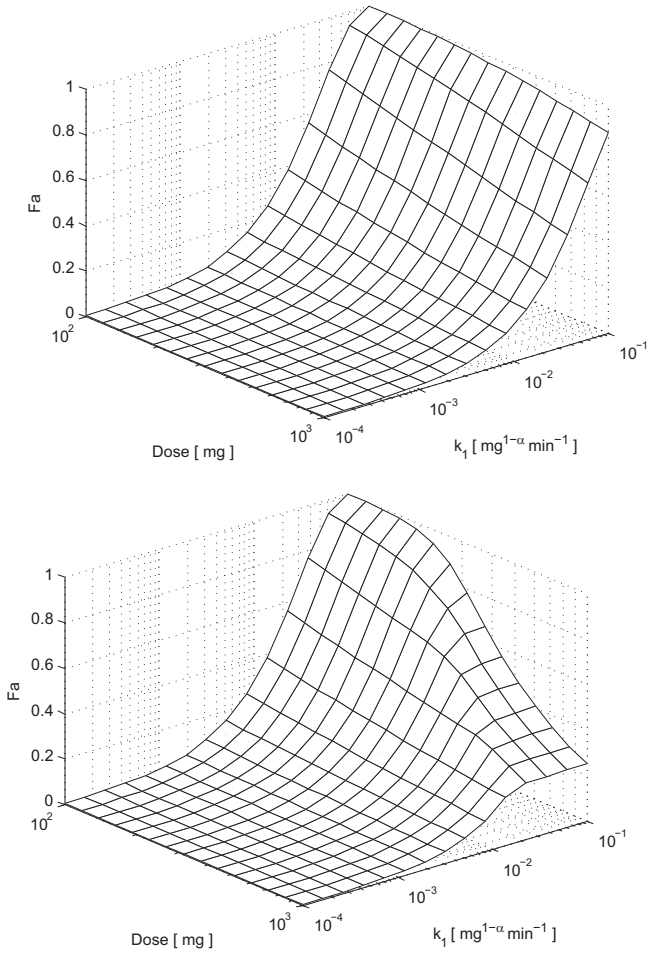

Fig. 3. Simulations of $F_a(MITT)$ with $\alpha = 0.7$ as a function of k_1^* and D with $C_S = 1$ (top) and 0.05 mg/mL (bottom).

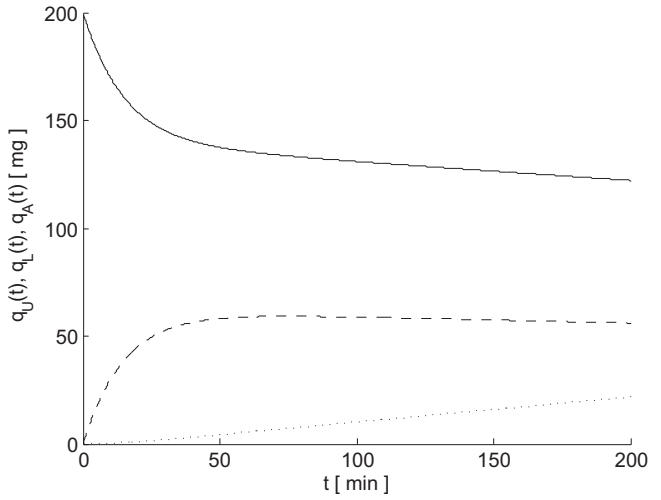

Fig. 4. Amount, time profiles for the undissolved (continuous curve), dissolved (dashed curve) and absorbed (dot curve) drug species assigning $D = 200$ mg, $k_{-1} = 0.050$ min^{-1}, $k_1^* = 0.1$ mg$^{1-\alpha}$min^{-1}, $C_S = 1$ mg/mL, $P_{eff} = 0.001$ cm/min and $\alpha = 0.7$.

extent of absorption ranges from 22 to 63 mg (11 and 31.5% of D, respectively) since a low value forP_{eff} was utilized in all cases.

Due to solubility limitations and the solubility constrain (Eq. (8)), all simulations (data not shown) for the amount, time profiles for all drug species of the insoluble drug ($C_S = 0.05$ mg/mL) exhibited limited dissolution assigning the parameters values reported in Figs. 4–6. In all

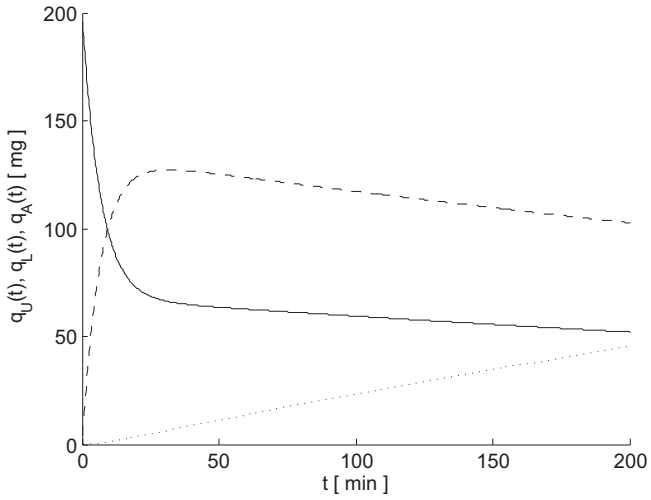

Fig. 5. Amount, time profiles for the undissolved (continuous curve), dissolved (dashed curve) and absorbed (dot curve) drug species assigning $D = 200$ mg, $k_{-1} = 0.050$ min^{-1}, $k_1^* = 0.1$ mg$^{1-\alpha} \cdot$ min^{-1}, $C_S = 1$ mg/mL, $P_{eff} = 0.001$ cm/min and $\alpha = 1$.

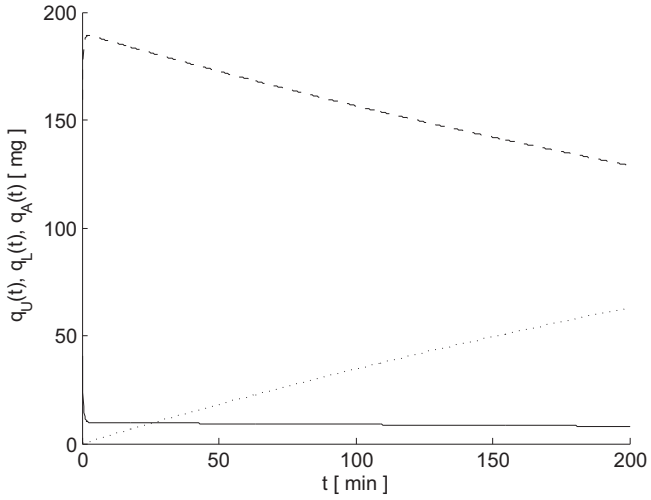

Fig. 6. Amount, time profiles for the undissolved (continuous curve), dissolved (dashed curve) and absorbed (dot curve) drug species assigning $D = 200$ mg, $k_{-1} = 0.050$ min^{-1}, $k_1^* = 0.1$ mg$^{1-\alpha} \cdot$ min^{-1}, $C_S = 1$ mg/mL, $P_{eff} = 0.001$ cm/min and $\alpha = 2$.

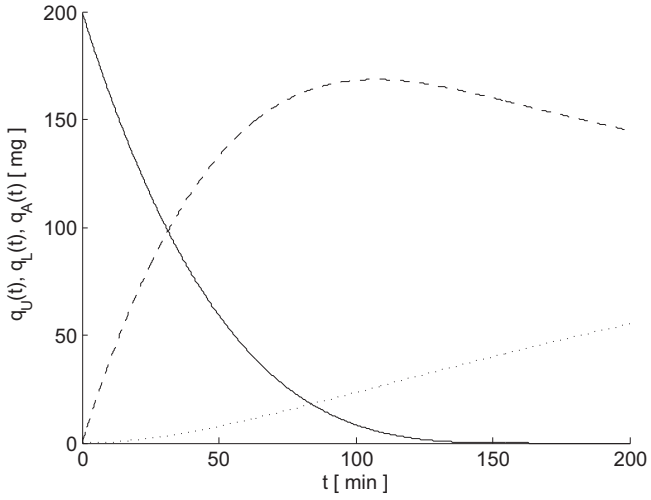

Fig. 7. Amount, time profiles for the undissolved (continuous curve), dissolved (dashed curve) and absorbed (dot curve) drug species assigning $D = 200$ mg, $k_{-1} = 0$, $k_1^* = 0.1$ mg$^{1-\alpha} \cdot$ min^{-1}, $C_S = 1$ mg/mL, $P_{eff} = 0.001$ cm/min and $\alpha = 0.7$.

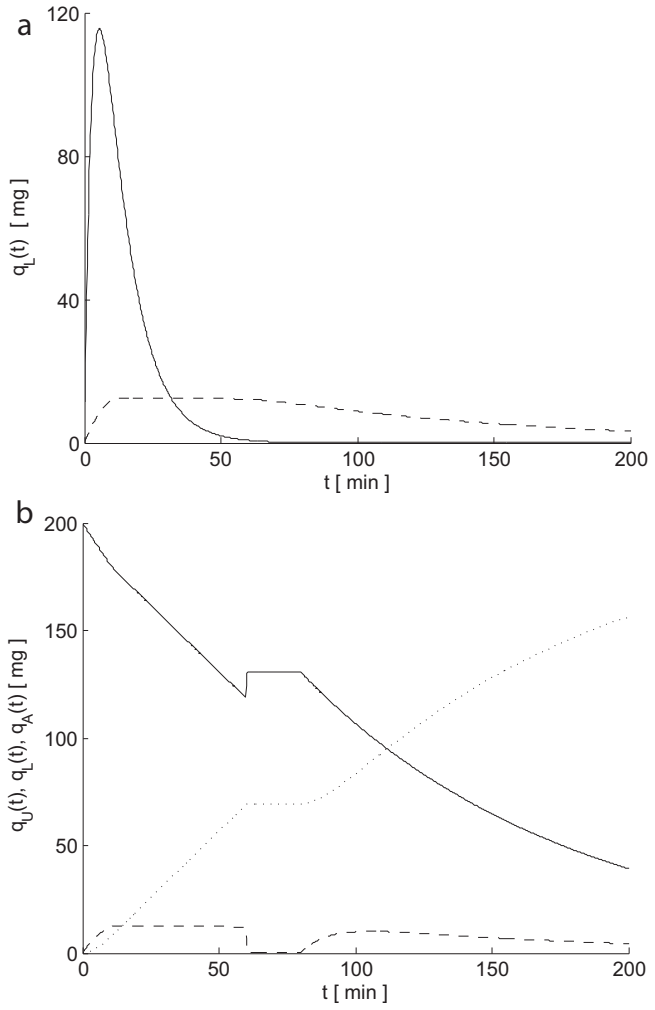

Fig. 8. (a) Amount, time profile (dashed curve) for the dissolved drug was generated using $\alpha = 1$, $C_S = 0.05$ mg/mL, $D = 200$ mg, $k_1^* = 0.01$ min^{-1}, $k_{-1} = 0$ min^{-1} and $P_{eff} = 0.005$ cm/ min ; the supersaturated $q_L(t)$ time profile (continuous curve) was generated using the same parameter values and assigning $k_1^* = 0.3$ min^{-1}, $C_S = 0.5$ mg/mL. Note that supersaturated data, $q_L(t) >$ (0.05 mg/mL) (250 mL) = 12.5 mg, which is the plateau value for the dashed curve, are maintained for 32 min. (b) Amount, time profiles for the undissolved (continuous curve), dissolved (dashed curve) and absorbed (dot curve) drug species for a very rapid precipitation ($k_{-1} = 10$ min^{-1}which operates only between 60 and 80 min); all other parameters take values: $\alpha = 1$, $C_S = 0.05$ mg/mL, $D = 200$ mg, $k_1^* = 0.01$ min^{-1}, $k_{-1} = 0$ min^{-1} and $P_{eff} = 0.005$ cm/min.

cases, most of the drug remains undissolved for the time course of the study ($MITT = 199$ min) while the amount absorbed was found to be < 8 mg.

It should be noted that the amount, time profiles for the undissolved, dissolved and absorbed drug are also dependent on k_{-1} value, which governs the precipitation step. Thus, Fig. 7 shows higher $q_L(t)$, lower $q_U(t)$ and higher $q_A(t)$ time profiles when compared to Fig. 4 using the same parameter values as in Fig. 4 and assigning $k_{-1} = 0$ min^{-1} *i.e.* no precipitation.

4.1. The RLMD captures the dynamics of supersaturation and precipitation phenomena in the GI lumen

According to the current guidelines (EMA, 2010; FDA, 2015), Class I drugs (highly soluble and permeable) are well characterized and specific dissolution requirements are quoted in the guidelines. On the contrary, the extensive absorption of many Class II drugs (low solubility, high permeability) cannot be explained on the solubility principles of BCS and the relevant dissolution criteria of the guidelines (Rinaki et al., 2004; Yazdanian et al., 2004). During the last two decades, extensive *in vitro* dissolution work has been focused on the use of biorelevant media to interpret drug absorption under fasted and fed state conditions (Bou-Chacra et al., 2017; Fotaki and Vertzoni, 2010). Numerous studies and a plethora of biorelevant media have been utilized to mimic *in vivo* dissolution and demonstrate the increased solubility and dissolution rate of Class II drugs in these media (Bou-Chacra et al., 2017). Despite the extensive work in this field of research, all results are explained on the basis of diffusion layer model of dissolution. Intuitively, one should expect a kind of interaction between the solid particles and the components of dissolution media as it is explained in (Charkoftaki et al., 2011). Moreover, supersaturation and precipitation phenomena, which are frequently encountered in dissolution studies, are routinely explained relying exclusively on diffusional principles, *i.e.*, the enhanced saturation (thermodynamic or kinetic) solubility drives the higher rate of dissolution. In our days, the oral bioavailability enhancement through supersaturation for poorly absorbed drugs is becoming very popular and the term “supersaturating drug delivery systems” has been coined for these formulations (Brouwers et al., 2009; Fong et al., 2017).

The *in vivo* model developed herein can capture the “interaction” of drug/formulation with the gastrointestinal fluids and most importantly the dynamics of supersaturation and precipitation phenomena associated with the dissolution process. In this context, two examples are presented in Fig. 8.

In the first example, we utilized the following model parameters $\alpha = 1$, $C_S = 0.05$ mg/mL, $D = 200$ mg, $k_1^* = 0.01$ min^{-1}, $k_{-1} = 0$ min^{-1} and $P_{eff} = 0.005$ cm/min to generate *in vivo* $q_L(t)$ time profiles for the formulation shown with the dashed line in Fig. 8a. Assuming that this formulation is tested in a “reactive” *in vivo* dissolution medium, a supersaturated dissolution curve was simulated, Fig. 8a, solid line; this was accomplished by applying a 3-fold increase for the dissolution-reaction rate constant, $k_1^* = 0.3$min^{-1}, and a simultaneous 10-fold increase for the saturation solubility, $C_S = 0.5$mg/mL. Fig. 8a illustrates the $q_L(t)$ time profile, which show that supersaturated dissolution data $q_L(t) >$ (0.05 mg/mL) (250 mL) = 12.5 mg, are maintained for 32 min, (Fig. 8a solid line).

Fig. 8b shows a case of a very rapid precipitation $k_{-1} = 10$ min^{-1}which operates for 20 min between 60 and 80 min; all other parameters take values $\alpha = 1$, $C_S = 0.05$mg/mL, $D = 200$ mg, $k_1^* = 0.01$ min^{-1}, $k_{-1} = 0$ min^{-1} and $P_{eff} = 0.005$ cm/min. This scenario mimics the sudden acid/base type precipitation associated with the reaction of the dissolved drug species with H^+ species frequently encountered in GI absorption studies. The amount, time profiles for the undissolved $q_U(t)$, dissolved $q_L(t)$ and absorbed $q_A(t)$ drug show a sudden change (increase or decrease at 60 min, which is maintained up to 80 min), Fig. 8b. One should also note the re-dissolution of drug after 80 min and the corresponding decrease in $q_U(t)$ and increase of $q_A(t)$ time profiles, Fig. 8b. All these changes result in double peaks in plasma concentration-time profiles, which are usually encountered in the literature.

In an analogous manner, one can also consider-analyze dissolution studies with drugs in polymorphic forms which exhibit metastable and stable solubility. Usually, when the metastable solubility is reached, precipitation starts operating; this can be modeled by shifting the value of k_{-1} from zero to a certain value. Further on, the transition towards the polymorphic form with stable lower solubility can be modeled in a similar manner.

A validation exercise, which relies on the fitting of the model to the available concentration, time data was not undertaken. Unfortunately, there no reliable drug concentration, time data in the gastrointestinal fluids measured at various time points. In addition, a combination of models based on diffusion- and reaction- limited dissolution seems to operate under *in vivo* conditions (Shekunov and Montgomery, 2016). Therefore, future GI modeling work should include both dissolution mechanisms.

4.2. Towards a new paradigm for the biopharmaceutic classification of drugs

The use of solubility and permeability as the key parameters for the current biopharmaceutic classification guidelines (EMA, 2010; FDA, 2015) rely on the classical passive consideration for both dissolution and permeation processes operating under *in vivo* conditions. (Amidon et al., 1995; Oh et al., 1993). According to the diffusion layer model of dissolution used for the development of BCS (Amidon et al., 1995; Oh et al., 1993), the saturation solubility drives the dissolution rate. Some concerns have raised for the proper biopharmaceutic classification of drugs in relation to the solubility estimates, namely, whether the determined values represent genuine equilibrium solubilities (*i.e.*, thermodynamic values) or whether they represent the values associated with a metastable condition (*i.e.*, kinetic values) (Box and Comer, 2008). In addition, the solubility/dose ratio has been proposed as a more reliable parameter for use in the BCS (Rinaki et al., 2003b) assuming that drug dissolution follows the diffusion layer model of dissolution.

The present work relies on an *in vivo* model of drug dissolution assuming a reaction limited approach. Visual inspection of the first of Eq. (9) reveals that the undissolved dose drives the dissolution rate, the permeability controls the uptake of drug while solubility acts as an upper cutoff limit for the drug concentrations in the lumen (Eq. (8)). It should be noted here that several aspects for the role of dose for classification purposes in the BCS has been pointed out previously (Bergström et al., 2014; Rinaki et al., 2003a); thus, the solubility/dose ratio was found to drive the dissolution rate in the diffusion layer model of dissolution (Rinaki et al., 2003a), the "critical dose" concept and a "dose-dependent BCS" have been proposed (Charkoftaki et al., 2012) and recently the change in the "highest dose strength" concept of the BCS EMA guideline (EMA, 2010) has been criticized (Daousani and Macheras, 2015; Sediq et al., 2014).

This analysis indicates that solubility is not the driving force for the dissolution rate if a reaction limited model of dissolution operates under *in vivo* conditions. Due to the lack of knowledge about the *in vivo* dissolution mechanisms, a model independent biopharmaceutic classification scheme would be more reasonable. For example, the current dissolution requirements (% of dose dissolved at a given time interval) of the relevant biopharmaceutical guidelines (EMA, 2010; FDA, 2015) can be used as sole model independent parameters for biopharmaceutical classification purposes. Coupling these parameters with % drug metabolized (a model independent parameter used in BDDCS (Wu and Benet, 2005)), a fully model independent biopharmaceutic classification scheme can be formulated, Fig. 9. Although an estimate for the dimensionless solubility/dose ratio can be derived easily, estimates for a plethora of drugs including the NSAIDs (ketoprofen, ibuprofen, indomethacin, naproxen) with different physicochemical properties are available in the literature *e.g.* see Table 1 in (Macheras and Karalis, 2014). It is worthy to mention that the role of dose for the diffusion limited dissolution model in the context of the classical BCS has been explained, including ibuprofen as an example of Class migration, by our group previously (Charkoftaki et al., 2012). Class migration is considered here too; it is associated with the supersaturated phenomena (see Fig. 10 and relevant text below).

The lack of knowledge for the *in vivo* dissolution mechanisms stated above is substantiated from the *in vitro* findings of (Shekunov and Montgomery, 2016). According to these authors "the contribution of surface kinetics (a synonym of reaction limited kinetics) appears to be significant constituting ~20% resistance to the dissolution flux in the compendial rotating disk apparatus at 100 rpm. The surface kinetics contribution becomes more dominant under condition of fast laminar or turbulent flows or in cases when the surface kinetics coefficient may decrease as a function of solution composition or pH." These findings based on experimental data available for approximately 100 compounds of pharmaceutical interest obtained under fully controlled conditions, indicate that the contribution of the two concurrent dissolution mechanisms vary in accord with the hydrodynamic conditions, the solution composition and pH. Accordingly, the contribution of the two mechanisms under *in vivo* conditions cannot either predicted or estimated using the current models since they are based exclusively on diffusion limited dissolution.

Based on the experience gained so far with the application of BCS for regulatory purposes, one can conclude that the extensive absorption of highly soluble drugs (Class I and Class III) is nicely explained on the basis of solubility estimates assuming the prevalence of the diffusion layer model of dissolution under *in vivo* conditions, Fig. 10, right hand side - abscissa. On the contrary, the extensive absorption of several Class II drugs *e.g.* NSAIDs (Yazdanian et al., 2004) cannot be explained on the basis of the classical solubility estimates and the dissolution criteria associated with the diffusion layer model of dissolution. On the contrary, the plethora of 'supersaturating drug delivery systems' (Brouwers et al., 2009; Fong et al., 2017) of Class II drugs exhibiting enhancement of bioavailability indicates that these drugs follow a reaction limited model of dissolution, Fig. 10, left hand side - abscissa. It should be emphasized that weak acids like NSAIDs were found (Fong et al., 2017) to exhibit the highest enhancement of bioavailability following the supersaturation concepts. These observations prompted us to propose a property (solubility) dependent dissolution mechanism in relation to the extent of drug's absorption, Fig. 10; plausibly, all drugs can be plotted in (the fraction absorbed, dimensionless solubility/dose ratio) plane of Fig. 10 provided that estimates for both variables are available. Needless to say that the dissolution mechanisms can coexist under *in vivo* conditions and the contribution of each one towards the

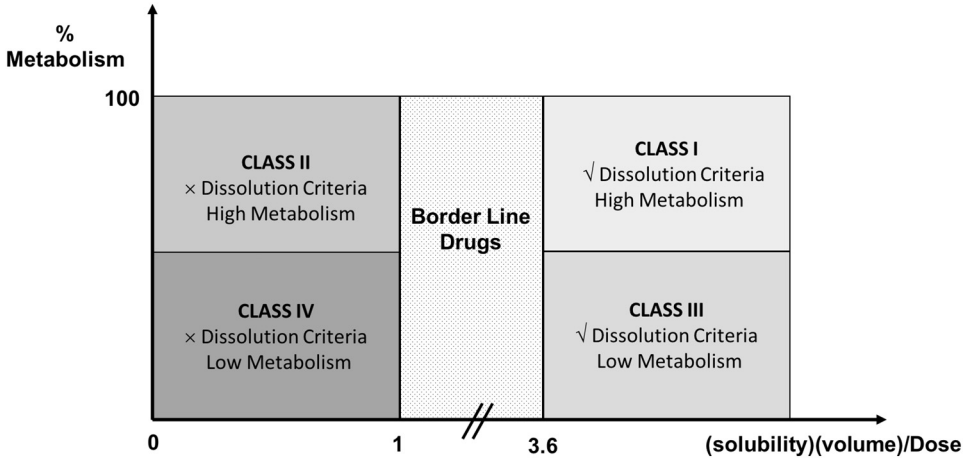

Fig. 9. A model independent biopharmaceutic classification system based on % metabolism (high, low) and the fulfillment (√) or not (x) of the current dissolution criteria. The dimensionless abscissa denotes the (solubility)·(volume)/dose values of drugs. The border line drugs lie between 1 and 3.6. These numbers correspond to drugs, which have solubility and dose values equal to the amount needed to saturate 250 mL (routinely used as the volume of gastrointestinal fluids) and 900 mL (the typical volume of the official dissolution tests) of water, respectively.

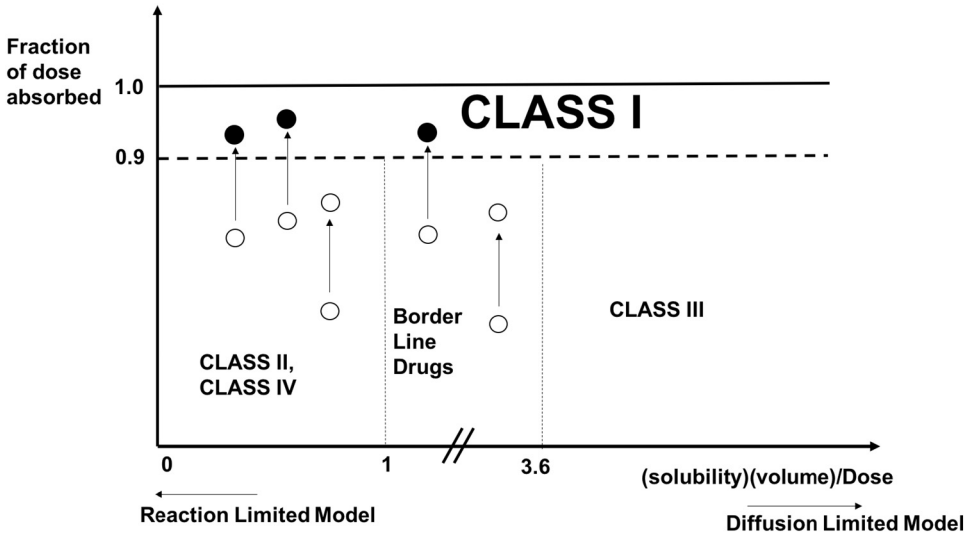

Fig. 10. Supersaturation can enhance the extent of absorption for Class II and IV drugs. This can either lead to class migration (•) (from Class II and IV and border line drugs to Class I) or not (○). The horizontal dashed line corresponds to the lower limit (0.9) for the fraction of dose absorbed of Class I drugs. Although the contribution of each one of the two dissolution mechanisms under *in vivo* conditions is unknown, the enhancement of bioavailability of insoluble compounds (Class II and IV), *via* supersaturation, seems to be associated with the reaction limited model of dissolution. For highly soluble drugs, the diffusion limited model of dissolution, because of the predominant role of solubility, describes adequately their classification in Class I and III. The two models are depicted schematically below the abscissa of the graph.

dissolution of drugs will remain a mystery for the many years to come.

The current BCS is often used not only for bioequivalence considerations but also in early development for an initial biopharmaceutical assessment of new drug candidates. Based on such an assessment or more advanced physiologically-based modeling, dissolution specifications are later defined. In parallel, regulatory bodies require a rational for setting dissolution specifications. The proposed classification (Fig. 9) is based on the current FDA and EMA dissolution requirements, which are re-named “dissolution criteria' for the biopharmaceutical classification purposes of this study. However, improvements in the understanding of the relevant supersaturation phenomena can help the modification and/or addition of the current experimental methodologies for more appropriate/advanced “dissolution requirements”. For example, the biorelevant dissolution work can be shifted towards media assessing the supersaturation behavior of compounds of pharmaceutical interest. New methodologies focusing on the relevant contribution of the two dissolution mechanisms under varying agitation conditions can be developed. The elegant work of (Shekunov and Montgomery, 2016) can be the starting point to better explain the difference of the dissolution-limitation *versus* assumed reaction-limitation when comparing the hydrodynamic situation in a compendial *in vitro* test *versus* an expected *in vivo* dissolution. The results of such studies can be further coupled with physiologically-based models to improve the predictive power of the models. Besides, computational approaches based on molecular descriptors or physicochemical properties can shed light on the supersaturation phenomena for Class II and IV drugs.

5. Conclusions

The reaction limited *in vivo* dissolution model developed can explain both classical, supersaturated concentration-time profiles including a precipitation phase too. The undissolved dose drives the dissolution rate while the saturation solubility acts as an upper limit for the concentration of drug in the GI lumen. The reaction limited model of dissolution (Eq. (9)) can be coupled with pharmacokinetic and disposition drug characteristics for the development of an integrated physiologically based model. Work is in progress towards this end.

Our ignorance regarding the exact dissolution mechanisms operating under *in vivo* conditions, prompted us to propose a model independent biopharmaceutic classification scheme of four drug categories based on the fulfillment or not of the current dissolution criteria and the high or low % drug metabolism. A buffer zone with border line drugs between Classes I/III and II/IV based on dimensionless (solubility)·(volume)/dose estimates, ensuring continuity in the classification, was also proposed. The extensive absorption of several current Class II, IV and borderline drugs is interpreted on the basis of the supersaturated dissolution behavior associated with the reaction limited *in vivo* dissolution model.

Acknowledgements

The authors would like to thank the anonymous reviewers for their constructive critisism. One of the authors (PM) would like to dedicate the article to undergraduate and graduate students who inspired him.

References

Amidon, G.L., Lennernäs, H., Shah, V.P., Crison, J.R., 1995. A theoretical basis for a biopharmaceutic drug classification: the correlation of in vitro drug product dissolution and in vivo bioavailability. Pharm. Res. 12, 413–420.

Anderson, R.A., Morgan, K.J., 1966. Effect of solubilisation on the antibacterial activity of hexachlorophane. J. Pharm. Pharmacol. 18, 449–456. http://dx.doi.org/10.1111/j.2042-7158.1966.tb07905.x.

Bergström, C.A.S., Andersson, S.B.E., Fagerberg, J.H., Ragnarsson, G., Lindahl, A., 2014. Is the full potential of the biopharmaceutics classification system reached? Eur. J. Pharm. Sci. 57, 224–231. http://dx.doi.org/10.1016/j.ejps.2013.09.010.

Bou-Chacra, N., Melo, K.J.C., Morales, I.A.C., Stippler, E.S., Kesisoglou, F., Yazdanian, M., Löbenberg, R., 2017. Evolution of choice of solubility and dissolution media after two decades of biopharmaceutical classification system. AAPS J. 19, 989–1001. http://dx.doi.org/10.1208/s12248-017-0085-5.

Box, K.J., Comer, J.E.A., 2008. Using measured pKa, LogP and solubility to investigate supersaturation and predict BCS class. Curr. Drug Metab. 9, 869–878.

Brouwers, J., Brewster, M.E., Augustijns, P., 2009. Supersaturating drug delivery systems: the answer to solubility-limited oral bioavailability? J. Pharm. Sci. 98, 2549–2572. http://dx.doi.org/10.1002/jps.21650.

Cardot, J.-M., Davit, B.M., 2012. In vitro–in vivo correlations: tricks and traps. AAPS J. 14, 491–499. http://dx.doi.org/10.1208/s12248-012-9359-0.

Charkoftaki, G., Dokoumetzidis, A., Valsami, G., Macheras, P., 2011. Supersaturated dissolution data and their interpretation: the TPGS-carbamazepine model case. J. Pharm. Pharmacol. 63, 352–361. http://dx.doi.org/10.1111/j.2042-7158.2010.01226.x.

Charkoftaki, G., Dokoumetzidis, A., Valsami, G., Macheras, P., 2012. Elucidating the role of dose in the biopharmaceutics classification of drugs: the concepts of critical dose, effective in vivo solubility, and dose-dependent BCS. Pharm. Res. 29, 3188–3198. http://dx.doi.org/10.1007/s11095-012-0815-4.

Cheow, W.S., Kiew, T.Y., Yang, Y., Hadinoto, K., 2014. Amorphization strategy affects the stability and Supersaturation profile of amorphous drug nanoparticles. Mol. Pharm. 11, 1611–1620. http://dx.doi.org/10.1021/mp400788p.

Crisp, M.T., Tucker, C.J., Rogers, T.L., Williams, R.O., Johnston, K.P., 2007. Turbidimetric measurement and prediction of dissolution rates of poorly soluble drug nanocrystals. J. Control. Release 117, 351–359. http://dx.doi.org/10.1016/j.jconrel.2006.11.011.

Daousani, C., Macheras, P., 2015. Scientific considerations concerning the EMA change in the definition of “dose” of the BCS-based biowaiver guideline and implications for bioequivalence. Int. J. Pharm. 478, 606–609. http://dx.doi.org/10.1016/j.ijpharm.2014.11.062.

Dokoumetzidis, A., Macheras, P., 2006. A century of dissolution research: from Noyes and Whitney to the biopharmaceutics classification system. Int. J. Pharm. 321, 1–11. http://dx.doi.org/10.1016/j.ijpharm.2006.07.011.

Dokoumetzidis, A., Macheras, P., 2009. Fractional kinetics in drug absorption and disposition processes. J. Pharmacokinet. Pharmacodyn. 36, 165–178. http://dx.doi.org/

10.1007/s10928-009-9116-x.
Dokoumetzidis, A., Papadopoulou, V., Valsami, G., Macheras, P., 2008. Development of a reaction-limited model of dissolution: application to official dissolution tests experiments. Int. J. Pharm. 355, 114–125. http://dx.doi.org/10.1016/j.ijpharm.2007.11.056.
EMA, 2010. Guideline on the Investigation of Bioequivalence. London.
FDA, 2015. "Guidance for industry: Waiver of In Vivo Bioavailability and Bioequivalence Studies for Immediate-Release Solid Oral Dosage Forms Based on a Biopharmaceutics Classification System," Food and Drug Administration. Rockville, MD.
Fong, S.Y.K., Bauer-Brandl, A., Brandl, M., 2017. Oral bioavailability enhancement through supersaturation: an update and meta-analysis. Expert Opin. Drug Deliv. 14, 403–426. http://dx.doi.org/10.1080/17425247.2016.1218465.
Fotaki, N., Vertzoni, M., 2010. Biorelevant dissolution methods and their applications in in vitro-in vivo correlations for oral formulations. Open Drug Deliv. J. 4, 2–13. http://dx.doi.org/10.2174/1874126601004020002. (~!2009-09-14~!2009-11-02~!2010-04-29~!).
González-García, I., Mangas-Sanjuán, V., Merino-Sanjuán, M., Bermejo, M., 2015. *In vitro–in vivo* correlations: general concepts, methodologies and regulatory applications. Drug Dev. Ind. Pharm. 41, 1935–1947. http://dx.doi.org/10.3109/03639045.2015.1054833.
Greco, K., Bogner, R., 2012. Solution-mediated phase transformation: significance during dissolution and implications for bioavailability. J. Pharm. Sci. 101, 2996–3018. http://dx.doi.org/10.1002/jps.23025.
Griffith, D.P., Bragin, S., Musher, D.M., 1976. Dissolution of struvite urinary stones. Experimental studies in vitro. Investig. Urol. 13, 351–353.
Higuchi, W.I., 1967. Diffusional models useful in biopharmaceutics. Drug release rate processes. J. Pharm. Sci. http://dx.doi.org/10.1002/jps.2600560302.
Holzbach, R.T., Pak, C.Y.C., 1974. Metastable supersaturation. Am. J. Med. 56, 141–143. http://dx.doi.org/10.1016/0002-9343(74)90590-7.
de Ilarduya, M.C.T., Martían, C., Goñi, M.M., Martínez-Ohárriz, M.C., 1998. Solubilization and interaction of sulindac with β-cyclodextrin in the solid state and in aqueous solution. Drug Dev. Ind. Pharm. 24, 301–306. http://dx.doi.org/10.3109/03639049809085624.
Jakubiak, P., Wagner, B., Grimm, H.P., Petrig-Schaffland, J., Schuler, F., Alvarez-Sánchez, R., 2016. Development of a unified dissolution and precipitation model and its use for the prediction of oral drug absorption. Mol. Pharm. 13, 586–598. http://dx.doi.org/10.1021/acs.molpharmaceut.5b00808.
Khan, J., Rades, T., Boyd, B., 2016. The precipitation behavior of poorly water-soluble drugs with an emphasis on the digestion of lipid based formulations. Pharm. Res. 33, 548–562. http://dx.doi.org/10.1007/s11095-015-1829-5.
Klein, S., 2010. The use of biorelevant dissolution media to forecast the in vivo performance of a drug. AAPS J. 12, 397–406. http://dx.doi.org/10.1208/s12248-010-9203-3.
Kopelman, R., 1988. Fractal reaction kinetics. Science 241, 1620–1626. http://dx.doi.org/10.1126/science.241.4873.1620. (80-.).
Kytariolos, J., Dokoumetzidis, A., Macheras, P., 2010. Power law IVIVC: an application of fractional kinetics for drug release and absorption. Eur. J. Pharm. Sci. 41, 299–304. http://dx.doi.org/10.1016/j.ejps.2010.06.015.
Levich, V., 1962. Physicochemical Hydrodynamics. Prentice-Hall, Englewood Cliffs N.J.
Li, C., Yu, D.-G., Williams, G.R., Wang, Z.-H., 2014. Fast-dissolving core-shell composite microparticles of quercetin fabricated using a coaxial electrospray process. PLoS One 9http://dx.doi.org/10.1371/journal.pone.0092106. (e92106-e92106).
Macheras, P., Argyrakis, P., 1997. Gastrointestinal drug absorption: is it time to consider heterogeneity as well as homogeneity? Pharm. Res. 14, 842–847.
Macheras, P., Dokoumetzidis, A., 2000. On the heterogeneity of drug dissolution and release. Pharm. Res. http://dx.doi.org/10.1023/A:1007596709657.
Macheras, P., Iliadis, A., 2016. Modeling in Biopharmaceutics, Pharmacokinetics and Pharmacodynamics, Interdisciplinary Applied Mathematics. Springer International Publishing, Cham. http://dx.doi.org/10.1007/978-3-319-27598-7.
Macheras, P., Karalis, V., 2014. A non-binary biopharmaceutical classification of drugs: the ABΓ system. Int. J. Pharm. 464, 85–90. http://dx.doi.org/10.1016/j.ijpharm.2014.01.022.
Macheras, P., Kouparis, M., Tsaprounis, C., 1986. Drug dissolution studies in milk using the automated flow injection serial dynamic dialysis technique. Int. J. Pharm. 33, 125–136. http://dx.doi.org/10.1016/0378-5173(86)90046-3.
Niederquell, A., Kuentz, M., 2014. Biorelevant dissolution of poorly soluble weak acids studied by UV imaging reveals ranges of fractal-like kinetics. Int. J. Pharm. 463, 38–49. http://dx.doi.org/10.1016/j.ijpharm.2013.12.049.
Oh, D.M., Curl, R.L., Amidon, G.L., 1993. Estimating the fraction dose absorbed from suspensions of poorly soluble compounds in humans: a mathematical model. Pharm. Res. 10, 264–270.
Parikh, T., Sandhu, H.K., Talele, T.T., Serajuddin, A.T.M., 2016. Characterization of solid dispersion of itraconazole prepared by solubilization in concentrated aqueous solutions of weak organic acids and drying. Pharm. Res. 33, 1456–1471. http://dx.doi.org/10.1007/s11095-016-1890-8.
Pouton, C.W., 2006. Formulation of poorly water-soluble drugs for oral administration: physicochemical and physiological issues and the lipid formulation classification system. Eur. J. Pharm. Sci. 29, 278–287. http://dx.doi.org/10.1016/j.ejps.2006.04.016.
Rinaki, E., Dokoumetzidis, A., Macheras, P., 2003a. The mean dissolution time depends on the dose/solubility ratio. Pharm. Res. 20, 406–408.
Rinaki, E., Valsami, G., Macheras, P., 2003b. Quantitative biopharmaceutics classification system: the central role of dose/solubility ratio. Pharm. Res. 20, 1917–1925.
Rinaki, E., Dokoumetzidis, A., Valsami, G., Macheras, P., 2004. Identification of biowaivers among class II drugs: theoretical justification and practical examples. Pharm. Res. 21, 1567–1572. http://dx.doi.org/10.1023/B:PHAM.0000041450.25106.c8.
Sediq, A., Kubbinga, M., Langguth, P., Dressman, J., 2014. The impact of the EMA change in definition of "dose" on the BCS dose–solubility ratio: a review of the biowaiver monographs. J. Pharm. Sci. 103, 65–70. http://dx.doi.org/10.1002/jps.23769.
Shekunov, B., Montgomery, E.R., 2016. Theoretical analysis of drug dissolution: I. Solubility and intrinsic dissolution rate. J. Pharm. Sci. 105, 2685–2697. http://dx.doi.org/10.1016/j.xphs.2015.12.006.
Valsami, G., Macheras, P., 1995. Determination of fractal reaction dimension in dissolution studies. Eur. J. Pharm. Sci. 3, 163–169.
Verma, S., Rudraraju, V.S., 2015. Wetting kinetics: an alternative approach towards understanding the enhanced dissolution rate for amorphous solid dispersion of a poorly soluble drug. AAPS PharmSciTech 16, 1079–1090. http://dx.doi.org/10.1208/s12249-014-0281-x.
Vrbata, P., Berka, P., Stránská, D., Doležal, P., Lázníček, M., 2014. Electrospinning of diosmin from aqueous solutions for improved dissolution and oral absorption. Int. J. Pharm. 473, 407–413. http://dx.doi.org/10.1016/j.ijpharm.2014.07.017.
Wang, Y., Abrahamsson, B., Lindfors, L., Brasseur, J.G., 2012. Comparison and analysis of theoretical models for diffusion-controlled dissolution. Mol. Pharm. http://dx.doi.org/10.1021/mp2002818. (120417094737002-120417094737002).
Wenzel, C.F., 2009. Lehre von der Verwandschaft der Körper. Kessinger Pub.
Wu, C.-Y., Benet, L.Z., 2005. Predicting drug disposition via application of BCS: transport/absorption/elimination interplay and development of a biopharmaceutics drug disposition classification system. Pharm. Res. 22, 11–23.
Yazdanian, M., Briggs, K., Jankovsky, C., Hawi, A., 2004. The "high solubility" definition of the current FDA guidance on biopharmaceutical classification system may be too strict for acidic drugs. Pharm. Res. 21, 293–299. http://dx.doi.org/10.1023/B:PHAM.0000016242.48642.71.
Yu, L.X., Lipka, E., Crison, J.R., Amidon, G.L., 1996. Transport approaches to the biopharmaceutical design of oral drug delivery systems: prediction of intestinal absorption. Adv. Drug Deliv. Rev. 19, 359–376.